

Quasiequilibrium supersolid phase of a two-dimensional dipolar crystal

I. L. Kurbakov,¹ Yu. E. Lozovik,¹ G. E. Astrakharchik,² and J. Boronat²

¹*Institute of Spectroscopy, 142190 Troitsk, Moscow region, Russia*

²*Departament de Física i Enginyeria Nuclear, Universitat Politècnica de Catalunya, Campus Nord B4-B5, E-08034 Barcelona, Spain*

(Received 21 June 2010; published 9 July 2010)

We have studied the possible existence of a supersolid phase of a two-dimensional dipolar crystal using quantum-Monte Carlo methods at zero temperature. Our results show that the commensurate solid is not a supersolid in the thermodynamic limit. The presence of vacancies or interstitials turns the solid into a supersolid phase even when a tiny fraction of them are present in a macroscopic system. The effective interaction between vacancies is repulsive making a quasiequilibrium dipolar supersolid possible.

DOI: [10.1103/PhysRevB.82.014508](https://doi.org/10.1103/PhysRevB.82.014508)

PACS number(s): 05.30.Jp, 67.85.-d

I. INTRODUCTION

Quantum systems with a dominant dipolar interaction have received permanent interest from the recent achievement of a Bose-Einstein condensed state of chromium atoms with a large dipole moment.¹ The anisotropy of the dipole-dipole interaction leads to exciting quantum phases that have been recently observed in fully quantum systems.² The experimental confirmation of these predicted phases and the collapses induced by the attractive part of the interaction can be even better realized if the permanent dipole moment of the particles becomes larger. A promising system for this goal is a stable gas of ultracold heteronuclear molecules.³

If the quantum dipoles are confined in a two-dimensional (2D) plane and all the dipole moments are perpendicular to the plane, the interaction is always repulsive and therefore the system is stable at any density. Under such spatial and orientational restrictions one loses relevant features that can emerge when the attractive collapse is approached but, on the other side, the stability of the 2D geometry allows for the possible observation of a gas-solid quantum-phase transition at high densities.^{4,5} A 2D environment is currently devised in the field of cold quantum gases by very anisotropic traps where the confinement in one direction is so tight that the transverse motion is frozen to zero-point oscillations.⁶ Another physical system where this 2D setup is relevant is the one of indirect excitons composed by electrons and holes physically separated using two-coupled quantum wells.⁷⁻¹⁰ If the distance between the electron and hole layers is significantly smaller than the electron-electron and hole-hole distances the resulting excitons can be modeled as composite bosons with a dipole-dipole interaction.^{11,12}

Recent quantum Monte Carlo calculations at zero⁴ and finite temperature⁵ have shown that a 2D homogeneous phase of dipoles experiments a gas-solid phase transition when the density increases. The equation of state of this solid phase, which forms a triangular lattice as well as its main structure properties are already reported in these previous works. However, relevant questions such as the possible superfluid signal and/or condensate fraction of the zero-temperature dipolar crystal were not addressed so far. In fact, there is at present a renewed interest in the search of supersolid phases where off-diagonal long-range order and spatial-solid order are simultaneously present.¹³ Recently, nonclas-

sical rotational inertia, measured in torsional-oscillator experiments with solid ⁴He, has been interpreted as supersolid signatures.¹⁴

Within the framework of Bose-Hubbard Hamiltonians supersolid phases of dipolar-lattice bosons have already been predicted. Danshita and Sá de Melo¹⁵ identify exotic phases as checkerboard and striped supersolid phases by including in the model Hamiltonian the attractive part of the dipole-dipole interaction and Trefzger *et al.*¹⁶ find a pair-supersolid phase in a bilayer configuration. The emergence of supersolid states when dipolar bosons are confined in two-dimensional optical lattices is probably favored by the free tuning of the localization strength of the external lattice potential included in the model Hamiltonian. A different concern is the possible formation of a supersolid phase in a continuum system where a solid is formed at high density without the presence of any external localization potential. In this work, we present the study of supersolidity in 2D dipolar bosons at zero temperature using quantum-Monte Carlo methods that rely merely on the microscopic Hamiltonian.

In Sec. II, we review the quantum-Monte Carlo method used in this study and specific details of the numerical simulations carried out. The main results obtained, with special attention to the role of defects on the supersolid properties of the dipolar crystal, are contained in Sec. III. Finally, Sec. IV comprises the summary of our work and concluding remarks.

II. METHOD

The triangular crystal phase of dipolar bosons is studied by means of the diffusion-Monte Carlo (DMC) method that it is nowadays a standard tool for achieving ground-state solutions of many-boson systems at zero temperature.¹⁷ The starting point of the DMC method is the Schrödinger equation written in imaginary time

$$-\hbar \frac{\partial \Psi(\mathbf{R}, z)}{\partial z} = (H - E_r) \Psi(\mathbf{R}, z) \quad (1)$$

with an N -particle Hamiltonian

$$H = -\frac{\hbar^2}{2m} \sum_{i=1}^N \nabla_i^2 + \sum_{i<j}^N V(r_{ij}). \quad (2)$$

In Eq. (1), E_r is a constant acting as a reference energy

and $\mathbf{R} \equiv (\mathbf{r}_1, \dots, \mathbf{r}_N)$ is a *walker* in Monte Carlo terminology. In order to reduce the variance to a manageable level and fix the symmetry of the system, it is a common practice to use importance sampling by introducing a trial wave function $\psi(\mathbf{R})$. Then, the Schrödinger equation is rewritten for the wave function $\Phi(\mathbf{R}, z) = \Psi(\mathbf{R}, z)\psi(\mathbf{R})$ and solved in a stochastic form. In the limit $z \rightarrow \infty$ only the lowest energy eigenfunction, not orthogonal to $\psi(\mathbf{R})$, survives and then the sampling of the ground state is effectively achieved. Apart from statistical uncertainties, the energy of a N -body bosonic system is exactly calculated.

As all the dipole moments are perpendicular to the plane, the dipole-dipole potential is

$$V(r) = \frac{C_{dd}}{4\pi} \frac{1}{r^3}. \quad (3)$$

The constant C_{dd} depends on the nature of the dipole-dipole interaction and increases proportionally to the square of the individual dipole moment. As in previous work, we define characteristic units of length $r_0 = mC_{dd}/(4\pi\hbar^2)$ and energy $\mathcal{E}_0 = \hbar^2/(mr_0^2)$ in such a way that the properties of the system are governed by a dimensionless density nr_0^2 with n as the particle density. In a previous work,⁴ the crystal phase of dipoles was studied using for ψ a nonsymmetric model [Nosanow-Jastrow (NJ)] since the focus was the determination of the equation of state and the phase-transition point, issues in which implicit symmetrization is much less relevant. Obviously, the NJ trial wave function cannot be used in the present study since our goal is the determination of superfluid signals in the solid and that is only possible assuming particle indistinguishability. To this end, in the present work we use a symmetric model

$$\psi(\mathbf{R}) = \prod_{i<j} f(r_{ij}) \prod_{l=1}^{N_{cr}} \left[\sum_{i=1}^N g(r_{li}) \right] \quad (4)$$

that was first introduced in the study of solid ⁴He at zero temperature.¹⁸ In Eq. (4), $\mathbf{R} = \{\mathbf{r}_1, \dots, \mathbf{r}_N\}$, $f(r)$ is a two-body Jastrow correlation factor chosen as in Ref. 4, $g(r_{li}) = \exp[-\alpha(\mathbf{r}_i - \mathbf{r}_l)^2]$ and N_{cr} is the number of lattice sites of the triangular crystal structure. This model wave function in Eq. (4) makes compatible the spatial solid order and the symmetry under the interchange of particles avoiding the numerically unworkable use of permanents on top of the NJ wave function.

Coherence phenomena in the dipolar solid have been studied by calculating the one-body density matrix $\rho_1(r)$ and the superfluid fraction n_s/n . The function $\rho_1(r)$ approaches a constant at long distances, which is the condensate fraction $N_0/N = \lim_{r \rightarrow \infty} \rho_1(r)/n$, if off-diagonal long-range order exists in the system. In DMC, the function $\rho_1(r)$ cannot be calculated using a pure estimator and therefore some bias induced by the trial wave function ψ remains. To reduce this bias as far as possible the variational parameters entering in ψ have been optimized in such a way that the variational and DMC (mixed) estimations of N_0/N are coincident within their statistical errors. On the other hand, the superfluid density is computed by extending the winding-number technique, used in path-integral Monte Carlo simulations at finite

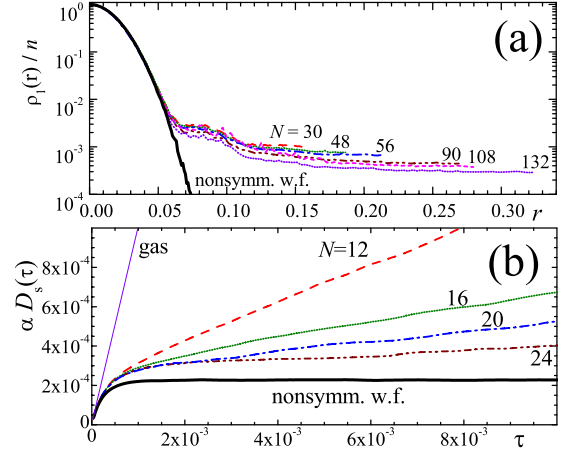


FIG. 1. (Color online) (a) One-body density matrix of the perfect 2D crystal at a density $nr_0^2 = 290$ and as a function of the number of particles N used in the simulation; the solid line corresponds to a nonsymmetric trial wave function. (b) The function $\alpha D_s(\tau)$, Eq. (5), at the same density and as a function of N ; the thin straight line corresponds to $n_s/n = 1$ and the solid line to the nonsymmetric case, $n_s/n = 0$.

temperature, to zero temperature.¹⁹ Explicitly

$$\frac{n_s}{n} = \lim_{\tau \rightarrow \infty} \alpha \left[\frac{D_s(\tau)}{\tau} \right], \quad (5)$$

where $\alpha = N/(4D_0)$ with $D_0 = \hbar^2/(2m)$, and $D_s(\tau) = \langle [\mathbf{R}_{CM}(\tau) - \mathbf{R}_{CM}(0)]^2 \rangle$ with \mathbf{R}_{CM} the center of mass of the particles and τ the imaginary time. Differently from the estimation of $\rho_1(r)$, the measure of the superfluid density in Eq. (5) is unbiased (pure estimator).

III. RESULTS

DMC results for the perfect 2D triangular solid are reported in Fig. 1. In all the simulations, carried out with different number of particles N , the one-body density matrix shows a plateau at long distances and therefore a finite condensate fraction. However, N_0/N decreases significantly with N making the condensate fraction vanishingly small in the thermodynamic limit $N \rightarrow \infty$. If the calculation is carried out with a nonsymmetric trial wave function (Nosanow-Jastrow model), $\rho_1(r)$ does not show off-diagonal long-range order for any value of N (see Fig. 1). We show in the same figure results for the superfluid density, plotting the function $\alpha D_s(\tau)$ [Eq. (5)] as a function of the imaginary time τ , the slope of this function is directly n_s/n . As one can see, the slope becomes zero within our numerical resolution for values $N \gtrsim 30$ pointing to the absence of supersolidity in the perfect crystal in the thermodynamic limit. The lack of supersolid signatures in the commensurate solid is observed at any density, starting on the melting one $n_m r_0^2 = 290(30)$ shown in Fig. 1.

The presence of defects or imperfections in a crystal has been suggested as a plausible explanation of the supersolid signals observed experimentally in torsional oscillator measurements of solid ⁴He. Whereas there are still open discus-

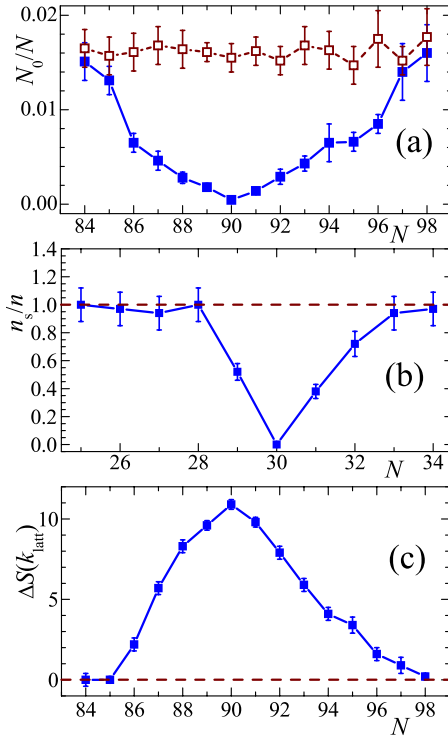


FIG. 2. (Color online) (a) Condensate fraction, (b) superfluid fraction, and (c) height of the main divergent peak of $\Delta S(k_{\text{latt}})$ with respect to the background at the reciprocal-lattice vector k_{latt} , for a crystal with vacancies or interstitials ($N \neq N_{\text{cr}}$) at density $nr_0^2=290$. Solid symbols with solid lines and open symbols with dashed lines stand for the solid and gas phases, respectively.

sions about the existence or not of vacancies in the ground state of bulk solid ^4He ,¹³ it seems very reasonable to think on the presence of vacancies or interstitials in a 2D crystal of dipoles. Indeed, indirect excitons or trapped atoms or molecules with high-dipole moments can be easily produced with a fraction of defects. We have collected in Fig. 2 DMC results for a dipolar solid with a finite fraction of vacancies or interstitials. Both the condensate fraction and superfluid density are very sensitive to the presence of defects: for any concentration of vacancies or interstitials a finite value for n_s/n and N_0/N is observed. When the fraction of vacancies is $\sim 6\%$ and $nr_0^2=290$, the supersolid melts: N_0/N equals its value in the gas phase, $n_s/n=1$, and the peak of $S(k)$ in the reciprocal-lattice vector disappears. The crystal also melts due to interstitials at a slightly higher concentration, $\sim 10\%$.

In Fig. 3, we show the density dependence of N_0/N , n_s/n , and height of the main peak of $S(k)$ for the particular case of one vacancy in a solid with $N_{\text{cr}}=30$. The condensate fraction becomes vanishingly small at high densities and remains always a factor of three to five smaller than its value in the gas phase, as also shown in the figure for comparison. The superfluid density fraction is $\sim 50\%$ at melting of the commensurate crystal and decreases with n but much more slowly than N_0/N . On the other hand, the height of the $S(k)$ peak increases with density as expected and it increases with N for a fixed n as it must be in a solid structure (not shown in the figure). At density $nr_0^2=230$ the supersolid completely melts: N_0/N becomes equal to its value in the gas, $n_s/n=1$, and the divergent peaks in $S(k)$ disappear.

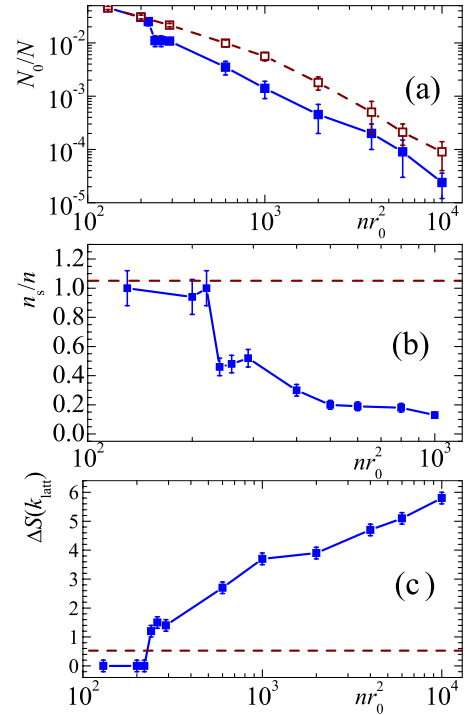


FIG. 3. (Color online) (a) Density dependence of the condensate fraction, (b) superfluid fraction, and (c) $S(k_{\text{latt}})$ peak for a solid with one vacancy. Solid and open points stand for the solid and gas phases, respectively.

As we commented before, the condensate fraction shows a significant dependence with N and therefore the estimation of the thermodynamic limit when vacancies are present is fundamental. For this purpose, we performed a study of the N dependence of N_0/N for vacancy fractions $0.018 \leq N_{\text{vac}}/N_{\text{cr}} \leq 0.042$. The DMC results obtained show a $1/N$ decrease with the number of Bose-condensed particles per vacancy, N_0/N_{vac} but with a finite value in the thermodynamic limit $N \rightarrow \infty$ of $N_0/N_{\text{vac}}=0.050(8)$. The number of superfluid particles per vacancy, which is weakly dependent on N , also remains finite in this limit. Also, the height of the narrow peak in $S(k)$ remains finite and proportional to N . Therefore, vacancy-induced superfluidity coexists with spatial solid order, i.e., a supersolid phase can exist.

A relevant concern about the stability of a small fraction of vacancies in the solid is the nature of their mutual interaction. Several microscopic estimations in solid ^4He show that two vacancies tend to form a weakly bound state because their interaction is attractive.^{20–22} Therefore, it has been argued that vacancies would form a cluster inside the crystal that eventually can evaporate producing a collapse of the crystal. In order to characterize the local structure of vacancies in a 2D dipolar crystal we have sampled the vacancy-vacancy two-body distribution function $g_{\text{vv}}(r)$. As vacancies are not *real* particles and our simulation works in a configuration space of particle coordinates one has to define what a vacancy position is for a given snapshot of the system. In our procedure, we have always identified a vacancy with one of the sites of the perfect triangular lattice in which unambiguously none of the particles is around it within a

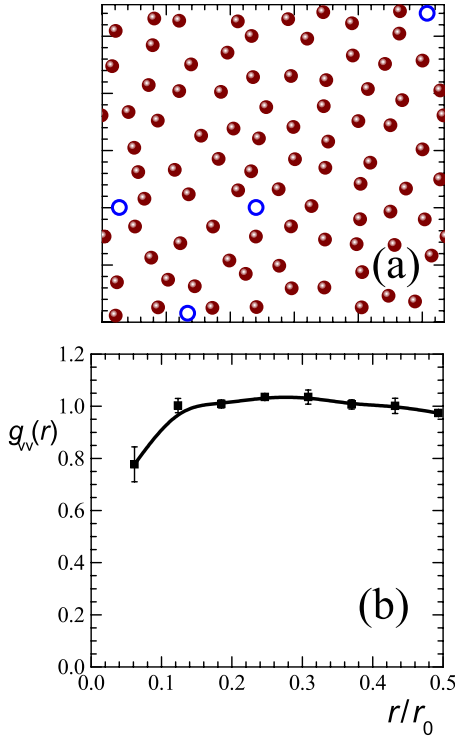


FIG. 4. (Color online) (a) Snapshot of a typical spatial configuration when vacancies are present. This case corresponds to $N_{\text{cr}}=90$ and $N=86$; crosses are the lattice points, solid circles are particles, and open circles, vacancies. (b) Vacancy-vacancy pair distribution function $g_{\text{vv}}(r)$ for the same N_{cr} and N values as in (a); $L = \sqrt{N}/n$ is the size of the simulation box.

cut-off radius that is close to the value of the lattice constant. Along the evolution in imaginary time, there are configurations in which we cannot identify the vacancy sites due to intrinsic fluctuations; in these cases we do not accumulate statistics for $g_{\text{vv}}(r)$. In Fig. 4, we show a snapshot of the system where vacancy sites are identified according to our definition. In the same figure, the vacancy-vacancy correlation function $g_{\text{vv}}(r)$ is shown for a setup composed by $N_{\text{cr}}=90$ and four vacancies. The radial function $g_{\text{vv}}(r)$ is normalized at each distance dividing what accumulated in each bin by the corresponding output obtained in a merely random distribution. As shown in Fig. 4(b), vacancies repel at short distances and this relevant feature is not only observed for this particular set of parameters but settled at other densities and vacancy fractions (below the threshold for melting). The repulsive interaction between vacancies in the 2D dipolar solid is probably due to the monotonously repulsive interaction between aligned dipoles that makes configurations to be more stable when vacancies spread in the system in order to effectively reduce the dipolar density. This is contrary to the vacancy-vacancy attraction observed in solid ^4He simulations in which the van der Waals attraction at long distances can explain the difference with the present results.

The ground state of the dipolar solid is a commensurate phase, i.e., without vacancies and/or interstitials. In other words, an activation energy is needed to create a vacancy or interstitial. We have estimated the activation energy to create one or more vacancies or interstitials using the DMC

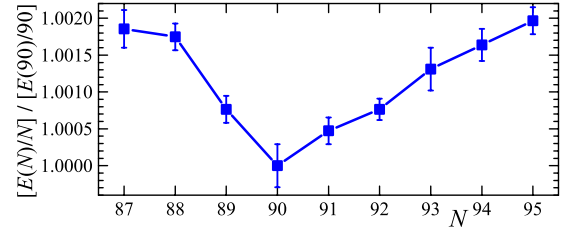


FIG. 5. (Color online) Energy per particle of the 2D dipolar solid as a function of the number of vacancies or interstitials, at density $nr_0^2=290$ and $N_{\text{cr}}=90$, and normalized to the energy per particle of the commensurate crystal.

method. In Fig. 5, we show the energies per particle of a solid with defects normalized to the energy per particle of the commensurate solid and having rescaled the simulation box size to work at fixed density. Our results support the metastability of the solid with defects with respect to the commensurate solid. The activation energy for the creation of a vacancy is higher than the corresponding one for an interstitial and this is maintained when the number of defects increases: the slopes of the two cases are rather different (see Fig. 5). It is worth noticing that this behavior is opposite to the one observed in solid ^4He where the activation energy for an interstitial is significantly larger than for a vacancy. Defining the activation energy in the standard way,²³ we get for one vacancy $E_v=2150(150)$ and for one interstitial $E_i=990(50)$, both at fixed density $nr_0^2=290$. These activation energies are significantly larger than the Berezinskii-Kosterlitz-Thouless temperature $T=380$,⁵ hindering thermal activation of defects.

IV. CONCLUDING REMARKS

In the present work, we have studied the possible emergence of bosonic-coherence phenomena in a two-dimensional crystal of dipoles by calculating the condensate fraction and superfluid density using accurate quantum-Monte Carlo methods. To this end, we have used in this system a trial wave function for importance sampling with both boson symmetry and solid order. Our DMC results show that the commensurate solid is not a supersolid since both n_s/n and N_0/N become zero in the thermodynamic limit within our numerical resolution. The introduction of defects, in the form of vacancies or interstitials, produces a dramatic effect on both quantities, even with tiny concentrations. A quasiequilibrium solid with vacancies or interstitials is proven to be supersolid within a predicted fraction of defects. If this percentage is further increased the supersolid melts.

The effective vacancy-vacancy interaction is repulsive at short distances, a feature that is opposite to the one of solid ^4He and that can help to stabilize the dipolar supersolid phase. The recrystallization to the ground state with a small fraction of defects is exponentially suppressed by the tunneling barrier which stabilizes a dipolar supersolid. Possible experimental realizations of a quasiequilibrium dipolar supersolid with defects include: (i) harmonically trapped dipolar molecules²⁴ or atoms²⁵ spatially localized with an optical

lattice and (ii) Wannier-Mott 2D dipolar excitons in single or coupled semiconductor quantum wells in electric and magnetic fields which are perpendicular to the quantum wells plane.²⁶ In the latter case, the finite excitation lifetime caused by their optical recombination gives rise to a continuous addition of vacancies into the system, resulting in a macroscopic supersolid at low temperatures.

ACKNOWLEDGMENTS

We wish to thank partial financial support from DGI (Spain) under Grant No. FIS2008-04403, Ramón y Cajal Program, and Generalitat de Catalunya under Grant No. 2009SGR-1003 is also acknowledged.

-
- ¹A. Griesmaier, J. Werner, S. Hensler, J. Stuhler, and T. Pfau, *Phys. Rev. Lett.* **94**, 160401 (2005).
- ²T. Lahaye, C. Menotti, L. Santos, M. Lewenstein, and T. Pfau, *Rep. Prog. Phys.* **72**, 126401 (2009).
- ³S. Y. T. van de Meerakker, H. L. Bethlem, and G. Meijer, *Nat. Phys.* **4**, 595 (2008).
- ⁴G. E. Astrakharchik, J. Boronat, I. L. Kurbakov, and Yu. E. Lozovik, *Phys. Rev. Lett.* **98**, 060405 (2007).
- ⁵H. P. Büchler, E. Demler, M. Lukin, A. Micheli, N. Prokof'ev, G. Pupillo, and P. Zoller, *Phys. Rev. Lett.* **98**, 060404 (2007).
- ⁶A. Görlitz, J. M. Vogels, A. E. Leanhardt, C. Raman, T. L. Gustavson, J. R. Abo-Shaeer, A. P. Chikkatur, S. Gupta, S. Inouye, T. Rosenband, and W. Ketterle, *Phys. Rev. Lett.* **87**, 130402 (2001).
- ⁷R. Rapaport, G. Chen, D. Snoke, S. H. Simon, L. Pfeiffer, K. West, Y. Liu, and S. Denev, *Phys. Rev. Lett.* **92**, 117405 (2004).
- ⁸J. P. Eisenstein and A. H. MacDonald, *Nature (London)* **432**, 691 (2004).
- ⁹S. Yang, A. T. Hammack, M. M. Fogler, L. V. Butov, and A. C. Gossard, *Phys. Rev. Lett.* **97**, 187402 (2006).
- ¹⁰A. V. Gorbunov and V. B. Timofeev, *JETP Lett.* **84**, 329 (2006).
- ¹¹Yu. E. Lozovik, O. L. Berman, and V. G. Tsvetus, *Phys. Rev. B* **59**, 5627 (1999).
- ¹²S. De Palo, F. Rapisarda, and G. Senatore, *Phys. Rev. Lett.* **88**, 206401 (2002).
- ¹³S. Balibar and F. Caupin, *J. Phys.: Condens. Matter* **20**, 173201 (2008).
- ¹⁴E. Kim and M. H. W. Chan, *Science* **305**, 1941 (2004).
- ¹⁵I. Danshita and C. A. R. Sá de Melo, *Phys. Rev. Lett.* **103**, 225301 (2009).
- ¹⁶C. Trefzger, C. Menotti, and M. Lewenstein, *Phys. Rev. Lett.* **103**, 035304 (2009).
- ¹⁷J. Boronat and J. Casulleras, *Phys. Rev. B* **49**, 8920 (1994).
- ¹⁸C. Cazorla, G. E. Astrakharchik, J. Casulleras, and J. Boronat, *New J. Phys.* **11**, 013047 (2009).
- ¹⁹S. Zhang, N. Kawashima, J. Carlson, and J. E. Gubernatis, *Phys. Rev. Lett.* **74**, 1500 (1995).
- ²⁰M. Boninsegni, A. B. Kuklov, L. Pollet, N. V. Prokof'ev, B. V. Svistunov, and M. Troyer, *Phys. Rev. Lett.* **97**, 080401 (2006).
- ²¹B. K. Clark and D. M. Ceperley, *Comput. Phys. Commun.* **179**, 82 (2008).
- ²²M. Rossi, E. Vitali, D. E. Galli, L. Reatto, and J. Phys., *J. Phys.: Conf. Ser.* **150**, 032090 (2009).
- ²³M. J. Gillan, *J. Phys.: Condens. Matter* **1**, 689 (1989).
- ²⁴B. Damski, L. Santos, E. Tiemann, M. Lewenstein, S. Kotochigova, P. Julienne, and P. Zoller, *Phys. Rev. Lett.* **90**, 110401 (2003).
- ²⁵K. Góral, K. Rzażewski, and T. Pfau, *Phys. Rev. A* **61**, 051601(R) (2000).
- ²⁶A. Filinov, P. Ludwig, Yu. E. Lozovik, M. Bonitz, and H. Stolz, *J. Phys.: Conf. Ser.* **35**, 197 (2006); Yu. E. Lozovik and A. M. Ruvinsky, *Sov. Phys. JETP* **85**, 979 (1997); *Phys. Lett. A* **227**, 271 (1997); Yu. E. Lozovik and V. I. Yudson, *Sov. Phys. JETP* **44**, 389 (1976).